Preprints of the 19th World Congress
The International Federation of Automatic Control
Cape Town, South Africa. August 24-29, 2014

A model-based prognosis strategy for prediction of Remaining Useful Life of Ball-Grid-Array Interconnections

David Gucik-Derigny * **Ali Zolghadri** * **Ephraim Suhir** **
Laurent Bechou *

* *University of Bordeaux-CNRS, IMS Lab 351 Cours de la Liberation, 33405 TALENCE Cedex, FRANCE. (e-mail: david.gucik-derigny@u-bordeaux1.fr, ali.zolghadri@ims-bordeaux.fr, laurent.bechou@u-bordeaux1.fr*
** *Portland State University, Portland, OR, USA, Technical University, Vienna, Austria, Ariel University, Ariel, Israel, and ERS Co., Los Altos, CA, 94024, USA, Tel. 650-969-1530, (e-mail: suhire@aol.com)*

Abstract: This paper deals with a model-based prognosis approach for assessing the remaining useful life (RUL) of a printed circuit board (PCB) subjected to impact or vibration loads applied to its support contour. The approach deals with the interaction (coupling) of the "fast" Ball-Grid-Array (BGA) vibration model and the "slow" low cycle fatigue damage model of BGA solder joint interconnections. As the complete knowledge of these interconnected models are typically not available, a two-stage filtering process is used to estimate the fast and slow dynamics involved. The RUL of the BGA solder joint interconnections is then estimated based on the identified models. Simulation results show the efficiency of the proposed approach.

Keywords: Prognosis, predictive diagnosis, RUL assessment, filtering, electronic system.

NOMENCLATURE

APS	Accumulated Plastic Strain
BGA	Ball-Grid-Array
EKF	Extended Kalman Filter
HOSM	High Order Sliding Modes
MIL	Military
PCB	Printed Circuit Board
RUL	Remaining Useful Life

1. INTRODUCTION

In avionics and aerospace electronics-rich systems, electronic components present substantial challenges to Prognostic and Health Monitoring/Management designers. Dynamic loading are applied on electronic devices during normal operation. Vibration, shock and drop loadings could have some significant effects on potential faults appearance and is part of MIL-specs JEDEC Standard (2001), JEDEC Standard (2003) during the device design stage. Devices availability at a certain performance level is crucial to be maintained in operational condition. On systems, health monitoring processes are designed with various monitoring strategies depending on the available information on systems.

In this paper, a PCB subjected to impact and vibration loads applied to its support contour is considered. A prognosis methodology is developed to estimate the RUL of the BGA solder joint interconnections, which is the most critical element of the PCB assembly. In the open literature, numerous works are dedicated to model the dynamic response of electronics systems experiencing shocks and vibrations Suhir et al. (2011a). The interested reader can refer to Suhir (2010a) for a complete state of the art review on the subject and the references quoted therein. Other works investigate PCB failure oriented accelerated testing Suhir (2010b), Suhir (2012) and PCB shocks protection adequate need Goyal et al. (1997), Huang et al. (2000), Lim et al. (2002). This paper proposes to combine the model-based system mechanics and damage behavior modelling in order to design a prognosis technique for on-line health monitoring. In general, physicists analytical approaches for a BGA solder joint RUL estimate are mainly based on static accumulated damage model considerations per solicitation cycle (Paris-Erdogan and Coffin-Manson laws, generalized isotropic damage model per cycle, see Lemaitre et al. (2005), etc). These types of models present the great advantage of easy on-line implementation and easy integration in the health monitoring system. They are built using a number of assumptions concerning damage birth and propagation from microscale to macroscale levels, and also for microdefects interactions in material. Moreover, the RUL estimation accuracy obtained is highly dependent on the damage initial condition knowledge, which is often not available. On the other hand, generally, physicists numerical approaches for BGA solder joint RUL estimate, based on Finite Element Analysis coupled with differential equation of damage model, assess better accurate RUL results than with the previous analytical ones. However, these types of models are hard to implement on-line due to high computational burden, even if damage behavior

modelling level is more accurate. The above considerations motivates an intermediate analytical predictive multiple time scale modelling which can be used for RUL estimation.

The paper is organized as follows. Section 2 introduces the PCB behavior model experiencing vibration or impact loads, coupled with a low cycle fatigue damage model for the BGA solder joint interconnections. Section 3 describes the proposed model-based prognosis for estimating RUL BGA solder joint interconnections. Section 4 presents some simulation results on the electronic system in order to show the efficiency of the proposed approach. Finally, some concluding remarks are given in Section 5.

2. DYNAMIC MODEL OF THE ELECTRONIC SYSTEM

In this section, an analytical model for a PCB carrying SMD through BGA solder joint interconnections and experiencing vibration and impact loads on its support contour is introduced. The proposed model is inspired from Suhir et al. (2009) characterising a nonlinear dynamic response of a PCB without SMD. It has the particular advantages to include explicitly and in a compact way the structure of the major model parameters (amplitude, frequency, stress, strain, etc) and their effects on PCB dynamic response. The model is based on the assumption that the PCB's contour is non-deformable, so that in-plane ("membrane") forces occur during the board vibrations which are highly nonlinear with a high frequency. Furthermore, the analysis is approximated and restricted to the first mode of vibrations, such that Duffing-type equation models the PCB dynamic response in the principal coordinate. This section proposes a more complete and detailed model than the one proposed in Suhir et al. (2009), by including the assembly solder joint material, BGA and SMD effect on the slowly drifting PCB damping parameter and integrating a low cycle fatigue BGA solder joint damage model. It includes the slow dynamics of damage effect that is coupled to the fast dynamics of the PCB.

The electronic system components are depicted in figure 1.

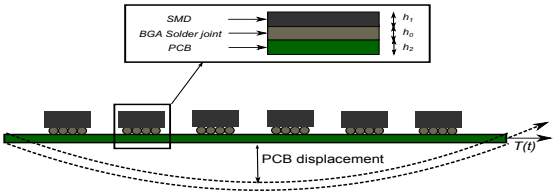

Fig. 1. Electronic system scheme

2.1 Shear stress/strain for BGA solder joint

Shear stress and strain are crucial for the damage dynamics model, because shear stress traduces the relationship between tensile in-plane ("membrane") force applied to (acting in) the PCB and the way the BGA solder joint interconnections are experiencing shear stress. In addition, shear strain characterizes how the BGA solder joint interconnection material adapts itself to the shear stress from an elastic and plastic point of view.

Let axial compliance of the PCB be defined as

$$\lambda_2 = \frac{1-\nu_2}{E_2 h_2} \tag{1}$$

where E_2, ν_2 and h_2 denote respectively Young's modulus and Poisson's ratio of PCB material, and PCB thickness, see Suhir (2013).

Let also the axial compliance of the package SMD on PCB be designated as

$$\lambda_1 = \frac{1-\nu_1}{E_1 h_1} \tag{2}$$

where E_1, ν_1, h_1 represent respectively Young's modulus and effective Poisson's ratio of package material, and package thickness.

$\lambda = \lambda_1 + \lambda_2$ is the total axial compliance of chip-PCB assembly.

Let also $\kappa_0 = \frac{h_0}{G_0}$ be the interfacial compliance of solder joint with h_0 the solder joint height and G_0 the shear modulus of solder material. Similarly, $\kappa_1 = \frac{h_1}{G_1}$ defines the interfacial compliance of package with G_1 the effective shear modulus of package material and $\kappa_2 = \frac{h_2}{G_2}$ the interfacial compliance of the PCB with G_2 PCB effective shear modulus. We also define $\kappa = \kappa_0 + \kappa_1 + \kappa_2$ total interfacial compliance of the assembly and $k = \sqrt{\frac{\lambda}{\kappa}}$ is the interfacial shearing stress parameter.

From now on, $T(t)$, $t \in \mathbb{R}^+$, denotes the tensile in-plane ("membrane") force applied to the PCB, experiencing shock-excited vibrations, described by:

$$T(t) = \left(\frac{\pi}{4a}\right)^2 E_2 h_2 f^2(t) \tag{3}$$

where $f(t)$ denotes the PCB's displacement and a represents the PCB half length size. Its rate is deduced as

$$\dot{T}(t) = 2\left(\frac{\pi}{4a}\right)^2 E_2 h_2 f(t)\dot{f}(t). \tag{4}$$

Then, the shearing stress τ and shearing strain γ for BGA solder joint are now defined as:

$$\begin{cases} \tau(x,t) = k\dfrac{\lambda_2}{\lambda}T(t)\dfrac{sinh(kx)}{cosh(kl)} \\ \gamma(x,t) = \dfrac{\tau(x,t)}{G_0} \end{cases} \tag{5}$$

where x denotes the position belonging to the interval $[0,\ l]$, with l is the half of the package length.

Also, the shearing stress and strain rates are deduced as:

$$\begin{cases} \dot{\tau}(x,t) = k\dfrac{\lambda_2}{\lambda}\dot{T}(t)\dfrac{sinh(kx)}{cosh(kl)} \\ \dot{\gamma}(x,t) = \dfrac{\dot{\tau}(x,t)}{G_0} \end{cases}. \tag{6}$$

Remark 1: $x = l$ permits to estimate the maximum stress and strain for a BGA solder joint. In the sequel, $\tau(t)$ and $\gamma(t)$ correspond to $\tau(x = l, t)$ and $\gamma(x = l, t)$.

2.2 Low cycle fatigue damage model for BGA solder joint

Numerous models from damage mechanics theory were proposed in literature by physicists Lemaitre et al. (2005).

Considering the type of damage phenomenon embedded for the solder joint damage behavior, experiencing stress and strain loads, it is assumed that an isotropic low cycle fatigue damage model (see Lemaitre et al. (2005) chapter 4) describes the solder joint damage dynamics:

$$\dot{\phi}(t) = \begin{cases} 0 \text{ if } p < p_c \\ \left(\dfrac{G_0}{2S}\dfrac{\gamma^2(t)}{(1-\phi)^2}\right)^s \dot{p}(t) \text{ if } p \geq p_c \end{cases} \quad (7)$$

where $\dot{p}(t) = |\dot{\gamma}_p(t)|$ denotes the accumulated plastic strain (APS) rate, $p(t) = \int_{t_0}^{t} \dot{p}(t)$ designates the APS (damage incubation state) and p_c refers to the critical APS level from which a damage initiates at a macroscopic scale, depending on the considered material in BGA solder joint. We have also $\phi(t)$, solution of (7) such that $\phi \in [0,\ 1[$ that depicts the normalized damage state for BGA solder joint, S and s the temperature depending material parameters, and $\dot{\gamma}_p$ the shear plastic strain rate.

Let shear plastic strain rate be defined as:

$$\dot{\gamma}_p(t) = \frac{d}{dt}\left(\gamma(t) sin(\varpi t) exp(-k't)\right) \quad (8)$$

where ϖ and k' designate respectively the fundamental frequency of its free linear vibrations and the plastic strain intensity factor.

In the sequel, the effective strain is denoted as:

$$\tilde{\gamma}(t) = \frac{\gamma(t)}{1-\phi(t)}. \quad (9)$$

which corresponds to the increasing equivalent strain experienced by BGA solder joint interconnection as the damage increases.

2.3 PCB motion model

The PCB model without SMD introduced in Suhir et al. (2009) is recalled for clarity of the presentation below:

$$\ddot{f}(t) = -\varpi^2 f(t) - \mu f^3(t) + \frac{F}{M}u(t) \quad (10)$$

where $f(t),\ \dot{f}(t),\ \ddot{f}(t) \in \mathbb{R}$, refer to the principal coordinates of PCB dynamic response, respectively as the PCB displacement, velocity and acceleration. We have also μ, F and M denoting respectively the parameter of nonlinearity, the amplitude of PCB applied load and the PCB's mass. Furthermore, $u(t)$ designates the time depending input applied on the PCB.

From now on, PCB is experiencing harmonic vibration loads, $u(t) = B(t)sin(\Omega(t)t)$ where $B(t)$ and $\Omega(t)$ denote respectively time depending amplitude and frequency.

Now, effects of assembly solder joint material, BGA and SMD on the slowly drifting PCB damping parameter are taken into account and added to (10). Then, we get the following detailed model:

$$\ddot{f}(t) = -b(\gamma,\tilde{\gamma})\dot{f}(t) - \varpi^2 f(t) - \mu f^3(t) + \frac{F}{M}u(t) \quad (11)$$

where

$$b(\gamma,\tilde{\gamma}) = b_0 + \sum_{i=1}^{3} b_i \left(\int_{t_0}^{t} (\tilde{\gamma}(t) - \gamma(t))\, \mathrm{d}t\right)^{\frac{1}{i}} \quad (12)$$

corresponds to the time depending damping coefficient.

2.4 PCB assembly/damage model

Let $x_1(t) = f(t)$, $x_2(t) = \dot{f}(t)$ and $x_3(t) = \phi(t)$ and assuming that $x_1(t)$ and $\tilde{\gamma}(t)$ are measured. Then, the equivalent state space model for the PCB assembly model coupled with the BGA solder joint interconnection damage model is deduced:

$$\begin{cases} \dot{x}_1(t) &= x_2(t) + v_1 \\ \dot{x}_2(t) &= -b(\gamma,\tilde{\gamma})x_2(t) - \varpi^2 x_1(t) - \mu x_1^3(t) \\ &\quad + \dfrac{F}{M}u(t) + v_2 \\ \dot{x}_3(t) &= \begin{cases} \text{if } p \geq p_c \\ \left(\dfrac{G_0}{2S}\dfrac{\gamma^2(t)}{(1-x_3(t))^2}\right)^s |\dot{\gamma}_p(t)| + v_3 \end{cases} \\ y_1(t) &= x_1(t) + \omega_1 \\ y_2(t) &= \tilde{\gamma}(t) + \omega_2 \end{cases} \quad (13)$$

where v_i, $i = 1,2,3$ and ω_j, $j = 1,2$ represent respectively the i^{th} component state noise and the j^{th} component sensor noise. It is assumed that v_k and ω_k are both zero mean, stationary white sequences, Gaussian with covariance matrix

$$E\left[\begin{pmatrix}\omega_i \\ v_i\end{pmatrix}\begin{pmatrix}\omega_i^k & v_i^k\end{pmatrix}\right] = \begin{pmatrix}Q & S \\ S^i & R\end{pmatrix}\delta_{ik}, \quad (14)$$

where E denotes the expected value operator and δ is the Kronecker delta. It is assumed that $S = 0$ (no correlation between ω_k and v_k). Q and R are the covariance matrices associated to the state and measurement noises:

$$\begin{aligned} Q &= E\{v(k)v(k)^T\} \\ R &= E\{\omega_1(k)\omega_1(k)^T\}. \end{aligned} \quad (15)$$

As it will be seen later, Q and R play a crucial role in the filter design.

It is noteworthy that (13) is a MTSM with its fast dynamics part $(x_1,\ x_2)^T \in \mathbb{R}^2$ and its slow dynamics part $x_3 \in \mathbb{R}$. Since (13) has an unknown model part, the proposed methodology in the next section will estimate it and also the RUL of BGA solder joint interconnection.

3. PROGNOSIS METHODOLOGY

This section is devoted to the description of the proposed prognosis methodology. After definition the basic concepts, different steps involved in the prognosis strategy will be presented.

3.1 Basic concept

Assume that the time horizon is splitted into two time intervals as depicted in figure 2. Sensors acquire input and output observation measures on the electronic system during a time interval, named "analysis interval". Based

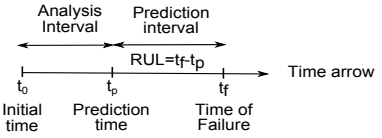

Fig. 2. Time split scheme

on observations during analysis interval $I_a = [t_0, t_p]$ with t_0 the initial time, a prediction is carried out at time t_p on interval $I_p =]t_p,\ \infty[$ to estimate the RUL of BGA solder

joint interconnection. The remaining useful life is defined as $t_{RUL} = t_f - t_p$ with t_f is the failure time at which $\phi(t_f) = \phi_c$, where ϕ_c denotes a critical damage level. For that, predictions are achieved under the hypothesis that future input model $u(t) \subset U \subset \mathbb{R}$ for $t \in]t_p,\ \infty[$ is assumed to be known a priori.
In the following, the prognosis problem is recasted into a well known reachability problem in control system theory Casti (1985).

Let $S \subset \mathbb{R}^3$ be the states set with $S = S_N \cup S_D$ where $S_N = \{(x_1\ x_2\ x_3)^T \in \mathbb{R}^3, \text{solution of (13)} \mid x_3 < \phi_c\}$ is the set of states relative to a normal functioning and $S_D = \{(x_1\ x_2\ x_3)^T \in \mathbb{R}^3, \text{solution of (13)} \mid x_3 \geq \phi_c\}$ is a set of state relative to a failure functioning. U designates the set of admissible controls at bounded value.

Let $U_0 \subset U$ such that $t_p < t_f$ and ν be an open of $\mathbb{R}^3$. $\varphi(t, t_0, S_0, U_0) : I_a \to \nu$ is a solution set of (13) from the initial conditions set $S_0 \subset S_N$ and the admissible control subset U_0 on time interval I_a.

The reached states set $\psi_{t_f}^{U_0}(S_0)$ at time t_f from the initial conditions set S_0 under admissible control subset U_0 is defined as:

$$\begin{aligned}\psi_{t_f}^{U_0}(S_0) = \{&\varphi(t_f, t_0, S_0, U_0), t_p < t_f \leq \infty,\\ &U_0 \subset U, S_0 \subset S_N\}\end{aligned} \tag{16}$$

The remaining useful life of the set S_D in a finite time is denoted by the following equality:

$$\begin{aligned}\mathrm{R}(t_f, S_D) = \{&S_0 \subset S_N | \exists U_0 \subset U, \exists t_f \in]t_p, \infty[,\\ &\varphi(t_f, t_0, S_0, U_0(.)) \subset S_D\}\end{aligned} \tag{17}$$

S_D is reached from S_0 if and only if

$$\psi_{t_f}^{U_0}(S_0) \cap S_D \neq \varnothing \tag{18}$$

If S_D is reached from S_0, the remaining useful life is designated as:

$$t_{RUL} = \inf_{t_f \in I_p} (\psi_{t_f}^{U_0}(S_0) \cap S_D \neq \varnothing) - t_p \tag{19}$$

3.2 Prognosis methodology steps

In this subsection, the proposed prognosis strategy for MTSM (13) is detailed and depicted in figure 3. It allows to reconstruct the unknown partial knowledge of (13) for estimating BGA solder joint interconnection RUL.

Firstly, the fast dynamics part analysis of (13) is derived based on observations on analysis interval I_a. Since state variables x_1 and x_2 are linked through an integrator chain (i.e $\dot{x}_1 = x_2$) and x_2 is non measurable, then a high order sliding modes (HOSM) differentiator Levant (2003) is used to estimate x_2. Moreover, the slowly drifting PCB damping parameter is estimated through the use of a divided difference filter Norgaard et al. (2000). Furthermore, BGA solder joint interconnection damage state is assessed from damage mechanics theory Lemaitre et al. (2005).
Secondly, the slow dynamics part analysis of (13) is achieved. For that, parameters S and s from the low cycle fatigue BGA solder joint damage model are estimated also on I_a, using a nonlinear least mean square algorithm. At this stage of the methodology, we estimate the unknown model part for (13), estimating finally the RUL of BGA solder joint interconnections assessment by simulation, on the time prediction interval I_p. It is based on the assumption of future input model knowledge a priori. Simulation is conducted until the critical level of state x_3 is reached at the corresponding time t_f. Each step is now more precisely explained.

Non-measured state x_2 estimate The first measurement y_1 is time derivating through the HOSM differentiator algorithm. For more details, the reader is referred to Levant (2003).

It enables to assess the shear strain rate $\dot{\gamma}(t)$ and its rate in (13). Based on (3), (4), (5), the following equalities are deduced:

$$\begin{aligned}\gamma(t) &= N y_1^2(t)\\ \dot{\gamma}(t) &= \frac{N}{2} y_1(t)\dot{y}_1(t)\end{aligned} \tag{20}$$

where $N = \dfrac{k\lambda_2\pi^2 E_2 h_2 sinh(kl)}{16 G_0 \lambda a^2 cosh(kl)}$.
Then, the plastic strain rate $\dot{\gamma}_p(t)$ is assessed in (8).

PCB damping parameter estimate Based on (12), PCB damping parameter estimate expression is rewritten as:

$$b(N y_1^2, y_2) = b_0 + \sum_{i=1}^{3} b_i \left(\int_{t_0}^{t} (y_2(t) - N y_1^2(t))\, \mathrm{d}t \right)^{\frac{1}{i}} \tag{21}$$

It is assumed that the damping parameter (22) can be approximated with a sufficient accuracy by the following form:

$$b \approx at + b_0 \tag{22}$$

where $at \approx \sum_{i=1}^{3} b_i \left(\int_{t_0}^{t} (\tilde{\gamma}(t) - \gamma(t))\, \mathrm{d}t \right)^{\frac{1}{i}}$.

The problem of estimating the parameter a is now addressed. Considering only the fast dynamics part of (13), let the augmented state vector be defined as $x = [x_1\ x_2\ a]^T$. Let also $v = [v_1\ v_2\ v_3]^T$ and $\omega = [\omega_1\ \omega_2]^T$, then the following model is derived:

$$\begin{cases}\dot{x}(t) &= f\left(x(t), u(t), \tilde{\gamma}(t), \gamma(t)\right) + v\\ y_1(t) &= x_1(t) + \omega_1\end{cases} \tag{23}$$

where the vector field f is defined as

$$f(.) = \begin{bmatrix} f_1\left(x(t), u(t), \tilde{\gamma}(t), \gamma(t)\right)\\ 0\end{bmatrix} \tag{24}$$

with $f_1(.) = \begin{bmatrix} x_2(t)\\ -b(\gamma, \tilde{\gamma}) x_2(t) - \varpi^2 x_1(t) - \mu x_1^3(t) + \dfrac{F}{M} u(t)\end{bmatrix}$.

The discrete-time state space model is deduced from (25) using a fourth order Runge Kutta method:

$$\begin{cases}x(k+1) &= \tilde{f}\left(x(k), u(k), \tilde{\gamma}(k), \gamma(k)\right) + v(k)\\ y_1(k) &= x_1(k) + \omega_1(k)\end{cases} \tag{25}$$

and the initial state and covariance matrix estimates are:

$$\begin{aligned}\bar{x}_0 &= E\{x_0\}\\ P_0 &= E\{(x - \bar{x}_0)(x - \bar{x}_0)^T\}\end{aligned} \tag{26}$$

Then the problem of recursively estimating state can be formulated as a nonlinear filtering problem Ljung et al. (1983). According to a specification of the uncertainties in model and measurements, the filter calculates an optimal estimation of the augmented state and its covariance matrix. A classical way to solve the filtering equations is to use the Extended Kalman Filter (EKF) Ljung et al. (1983).

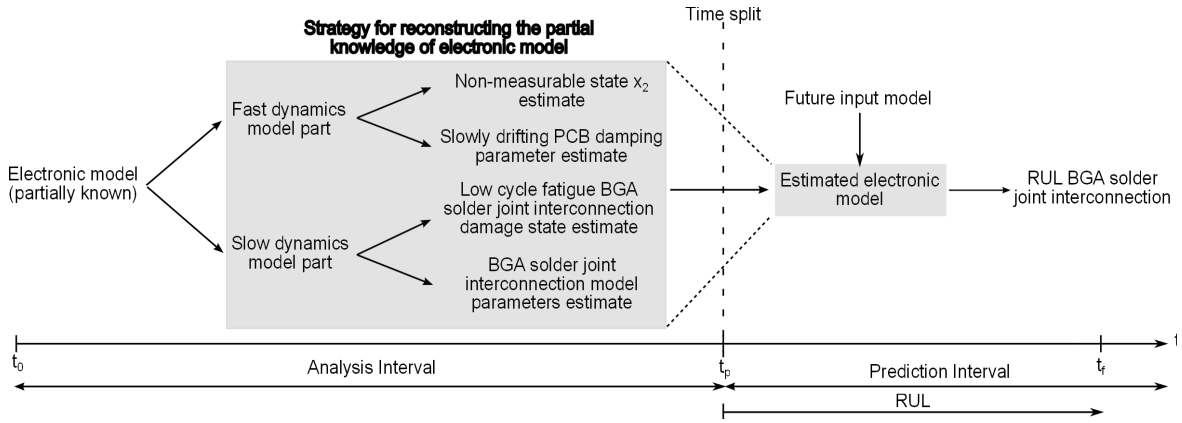

Fig. 3. Prognosis methodology for electronic system

The practical problems with the EKF are well-known, even when the hyper-parameters (Q and R) are well tuned. In Norgaard et al. (2000), the authors proposed a method based on polynomial approximation of the nonlinear approximations obtained with a multi-dimensional extension of Stirling's interpolation formula. In contrast to Taylor's formula, no derivatives are needed in the interpolation formula, only functions evaluations. This accommodates easy implementation and it is not necessary to assume differentiability of the nonlinear mappings. The method has been judged suitable and superior to the EKF in a wide range of applications; see for instance Zolghadri et al. (2004) and Zolghadri (2000). To avoid duplicating materials from Norgaard et al. (2000), the mechanization equations of the estimator are not given here, the interested reader can refer to Norgaard et al. (2000) for further details. To obtain correct results, the tuning of Q and R is a crucial issue. Note that in classical Kalman formulation, it is assumed that a complete a priori knowledge of the process and measurement noise statistics (Q and R) is available. Although these characteristics can be inferred from statistical and calibration procedures of the hardware sensing devices, the task is much more difficult for the process noise, because, in essence, it is usually used to represent modelling errors. Generally, a large Q or small R means a wide bandwidth. On the contrary, a small Q or large R represents a small bandwidth, i.e. the convergence speed is increased, but the filter may not follow the estimated quantities. In this study, the optimization of the hyper parameters is done by iteratively testing different values and evaluating the results over a test period.

Damage state estimation The second stage consists in assessing the slow dynamic damage state by an inversion method. For that, BGA solder joint interconnection damage is estimated from damage mechanics theory Lemaitre et al. (2005) (chap. 1). In most cases, the direct measure of damage state as the surface density of microdefects could not be carried out on-line by sensor and necessitates to be assessed through the coupling between damage and elasticity. In the case of isotropic damage, this coupling is defined as:

$$\tilde{\gamma}(t) = \frac{\tau(t)}{\tilde{G}_0} \tag{27}$$

where $\tilde{G}_0 = G_0(1-\hat{x}_3)$, with $\hat{x}_3$ the damage state estimate. Then the damage state is expressed as a loss of stiffness:

$$\begin{aligned} \hat{x}_3 &= 1 - \frac{\tilde{G}_0}{G_0} \\ &= 1 - \frac{\gamma(t)}{\tilde{\gamma}(t)} \end{aligned} \tag{28}$$

where $\gamma(t)$ is defined in (20) and $\tilde{\gamma}(t) = y_2(t)$. Finally, we get a additional fictitious output named $\hat{y}_3 = \hat{x}_3$.

BGA solder joint damage model estimate The parameter estimation problem for the damage model is now formulated. It is assumed that there exists a parameter vector $\hat{\theta} = \begin{bmatrix} \hat{\theta}_1 & \hat{\theta}_2 \end{bmatrix}^T \in \mathbb{R}^2$ such that a non-linear estimator defined as:

$$\begin{cases} \dot{\hat{\tilde{x}}}_3(t) = \left(\dfrac{G_0}{2\hat{\theta}_1} \dfrac{\gamma^2(t)}{(1-\hat{\tilde{x}}_3(t))^2} \right)^{\hat{\theta}_2} |\dot{\gamma}_p(t)| \\ \hat{\tilde{y}}_3 = \hat{\tilde{x}}_3 \end{cases} \tag{29}$$

for estimating the system damage state behavior (13) through observations on interval I_a. $\dot{\hat{x}}_3(t)$ is deduced from $\hat{x}_3(t)$ by using the HOSM differentiator introduced in Levant (2003).

RUL of BGA solder joint interconnection Based on the previous steps, an estimated electronic model is derived as:

$$\begin{cases} \dot{\hat{x}}_1(t) = \hat{x}_2(t) \\ \dot{\hat{x}}_2(t) = -\hat{b}\hat{x}_2(t) - \varpi^2 \hat{x}_1(t) - \mu \hat{x}_1^3(t) \\ \qquad\quad + \dfrac{F}{M} u(t) \\ \dot{\hat{\tilde{x}}}_3(t) = \begin{cases} \text{if } p \geq p_c \\ \left(\dfrac{G_0}{2\hat{\theta}_1} \dfrac{\hat{\gamma}^2(t)}{(1-\hat{\tilde{x}}_3(t))^2} \right)^{\hat{\theta}_2} |\dot{\hat{\gamma}}_p(t)| \end{cases} \\ \hat{y}_1 = \hat{x}_1(t) \\ \hat{y}_2 = \hat{\tilde{\gamma}}(t) \\ \hat{\tilde{y}}_3 = \hat{\tilde{x}}_3 \end{cases} \tag{30}$$

where

$\hat{\gamma}(t) = N\hat{y}_1^2(t)$ and $\dot{\hat{\gamma}}_p(t) = \dfrac{d}{dt}(\hat{\gamma}(t) sin(\varpi t) exp(-k't))$.

This model is used to assess the RUL of BGA solder joint interconnection on prediction interval I_p. From subsection 3.1, the RUL expression is deduced by an easy adaptation of the proposed prognosis definition concept to the model described by (30).

4. SIMULATION RESULTS

In this section, some simulation results are presented to illustrate the overall strategy.

Simulation results are obtained with a sampling frequency equal to 10KHz. All results are presented on normalized time scale, that is the total duration of the simulation experience is 1.

The following numerical values are used:

Par.	Value	Par.	Value
E_2	$2321.48kgf/mm^2$	E_1	$8775.5\ kgf/mm^2$
h_2	$1.5mm$	h_1	$2mm$
ν_2	0.3	ν_1	0.3
G_2	$892.7kgf/mm^2$	G_1	$3367.3kgf/mm^2$
h_0	$0.2mm$	G_0	$1958.8\ kgf/mm^2$
a	$150mm$	l	$15mm$
ϖ	$209.31s^{-1}$	μ	$25629.2\ mm^{-2}.s^{-2}$
F	$13.6kg$	M	$1.77.10^{-5}kgs^2/mm^2$
b_0	$5901s^{-1}$	p_c	10^{-3}
S	0.5	s	2

Table 1. Parameters value of electronic system

The initial state is:
$x_0 = [x_1(0)\ x_2(0)\ x_3(0)\ p(0)]^T = \left[0\ 0\ 10^{-3}\ 10^{-3}\right]^T$.

The PCB is experiencing harmonic vibration loads such that the input $u(t)$ depicted in figure 4 is a repeated sequence on intervals I_a and I_p. This input signal has the

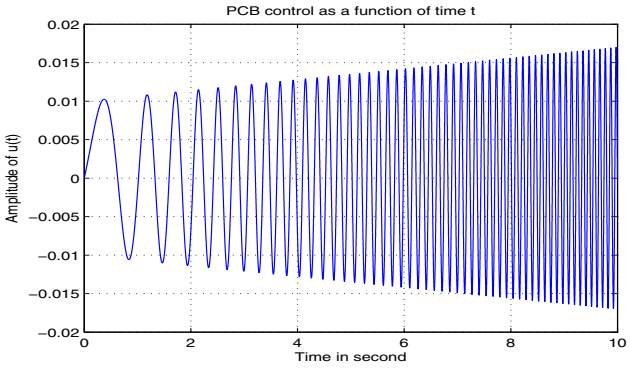

Fig. 4. PCB harmonic vibration loads

property to solicit the PCB oscillatory mode between 0.1 and 10Hz, frequencies interval which affects the most BGA solder joint damage.

4.1 Non-measured state x_2 estimate

The estimated state x_2 is illustrated in figure 5, which is a quite accurate estimate.

4.2 PCB damping parameter estimation

Figure 6 shows y_1 and $\hat{y}_1$ using the estimation of the damping parameter:

4.3 Damage state estimate

Applying the proposed methodology on the slow dynamics part model (13), the BGA solder joint damage state is

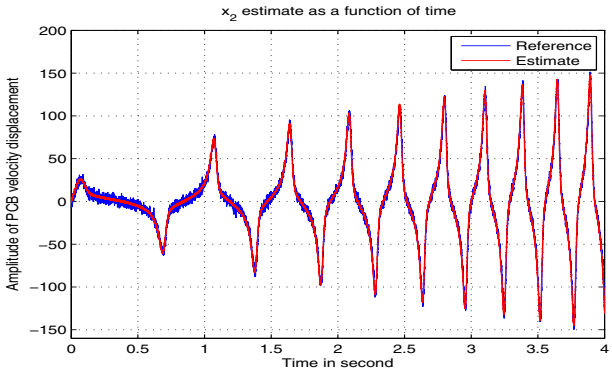

Fig. 5. Fast dynamic state estimate $\hat{x}_2$ vs x_2

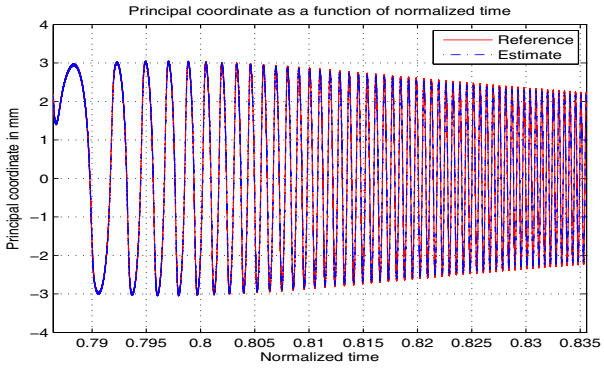

Fig. 6. Comparison between y_1 and $\hat{y}_1$ after damping parameter estimate

assessed from (7). Figure 7 presents the damage model estimation result.

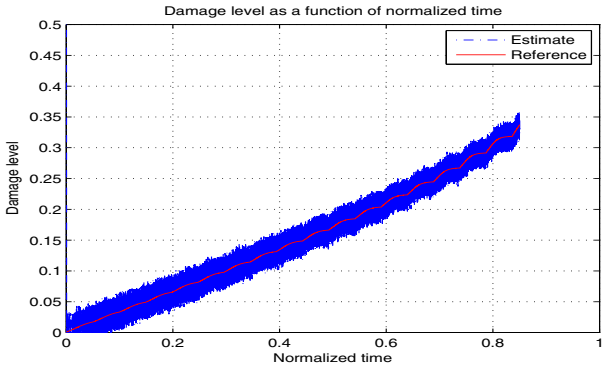

Fig. 7. Damage state estimate on analysis time interval $I_a = [0,\ 0.85]$

4.4 BGA solder joint damage model estimate

The next strategy step consists in assessing the BGA solder joint damage model from (30). Applying the non-linear least mean square algorithm, the figure 8 depicts the damage model estimate result. Based on the covariance knowledge of damping parameter estimate, upper and lower bounds for RUL estimate are derived.

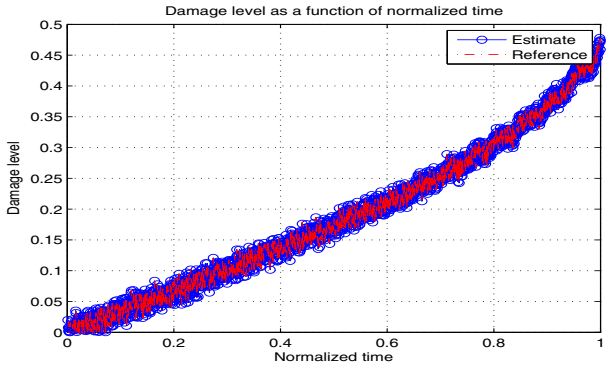

Fig. 8. Comparison between $\tilde{y}_3$ and $\hat{\tilde{y}}_3$ after damage model estimate

4.5 RUL of BGA solder joint interconnection

The last step of the proposed strategy is related to the RUL assessment on the prediction time t_p for a given interval time analysis $I_a = [0,\ 0.85]$.The RUL of BGA solder joint damage state and its bounds are assessed on prediction interval I_p based on (30) and an a priori knowledge of the future input model. The repeated sequence depicted in figure 4 is applied. The critical damage level is defined as 0.8. Then the RUL assessment result is illustrated in figure (9) and summed-up in the Table 2. For this situation, the proposed methodology gives accurate results of RUL estimate with 12% of uncertainty.

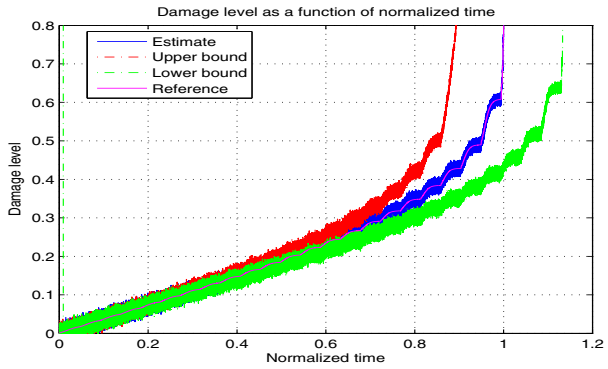

Fig. 9. BGA solder joint damage state prediction

Ref. RUL	Lower RUL	Est. RUL	Upper RUL
1	1.12	1	0.88

Table 2. RUL result on time prediction interval $I_a = [0,\ 0.85]$

5. CONCLUSION AND FUTURE WORKS

The problem studied in this paper is that of estimating the RUL of BGA solder joint interconnection. A prognosis strategy was developed and its efficiency was illustrated through simulation results where it has been noted that the proposed methodology succeeds to predict the RUL with about 12% of uncertainty. Further investigations are necessary to study the propagation of uncertainties in the estimated MTSM and its optimization on RUL assessment. Another appealing research direction is the extension of the proposed methodology by including set-membership approaches in order to build guaranteed upper and lower bounds for the RUL, based on available system uncertainties and disturbance bounds.

REFERENCES

J.L. Casti. Nonlinear system theory. *Mathematics in Science and Engineering*, volume 175, 1985.

S. Goyal, J.M Papadopoulos, and P.A. Sullivan, Shock Protection of Portable Electronic products: Shock Response Spectrum, Damage Boundary Approach, and Beyond. *Shock Vib.*, volume 4(3), 1997.

W. Huang, D.B. Kececiogl, and J.L. Prince. A simplified Random Vibration Analysis on Portable Electronic Products. *IEEE Trans. Compon. Packag. Technol.*, volume 3(3), pages 505–515, 2000.

Mechanical Shocks. *JEDEC Standard*, JESD22 B104 B, 2001.

Board Level Drop Test Method of Components for Handheld Electronic Products. *JEDEC Standard*, JESD22 B111, 2003.

J. Lemaitre, and R. Desmorat. Engineering Damage Mechanics: Ductile, Creep, Fatigue and Brittle Failures. *Springer*, 2006.

A.Levant. Higher-order sliding modes, differentiation and output-feedback control. *International Journal of Control*, volume 76(9), pages 924–941, 2003.

C.T. Lim, Y.M. Teo, and V.P.W. Shim. Numerical Simulation of the Drop Impact Response of a Portable Electronic Product. *IEEE CPMT Transactions*, volume 25(3), 2002.

L. Ljung, T. Soderstrom. Theory and practice of recursive identification. *MIT PRESS*, Cambridge, Mass. 1983.

M. Norgaard, N. Poulsen, and O. Ravn. New developments in state estimation for nonlinear systems. *Automatica*, volume 36(11), 2000.

E. Suhir, M. Vujosevic, and T. Reinikainen. Nonlinear dynamic response of a 'flexible-and-heavy' printed circuit board (PCB) to an impact load applied to its support contour. *Journal of Physics D: Applied Physics*, volume 42(4), 2009.

E. Suhir. Predictive Modeling of the Dynamic Response of Electronic Systems to Shocks and Vibrations. *Applied Mechanics Reviews*, volume 63(5), 2010.

E. Suhir. Probabilistic Design for Reliability. *Chips Scale Reviews*, volume 14(6), 2010.

E. Suhir, T.X. Yu, and D.S. Steinberg. Structural Dynamics of Electronic and Photonic Systems. *John Wiley and Sons*, Inc, 2011.

E. Suhir. When adequate and predictable reliability is imperative. *Microelectronics Reliability*, volume 52, pages 2342–2346, 2012.

E. Suhir. Predicted Size of an Inelastic Zone in a Ball-Grid-Array (BGA) Assembly. *IEEE Aerospace Conference*, pages 1–8, 2013.

A. Zolghadri, M. Monsion, D. Henry, C. Marcionini, and O. Petrique. Development of an operational model-based warning system for tropospheric ozone concentrations in Bordeaux, France. *Environmental Modelling and Software*, volume 19, pages 369–382, 2004.

A. Zolghadri. A redundancy-based strategy for safety management in a modern civil aircraft. *Control Engineering Practice*, volume 8(5), pages 545–554, 2000.